Uranium Removal from Ground Water Using Zero Valent Iron Media

by James Farrell[a], William D. Bostick[b], Robert J. Jarabek[b], and Joseph N. Fiedor[c]

Abstract

Removal of uranium from contaminated ground water using zero valent iron is currently under evaluation at several U.S. Department of Energy (DOE) facilities. Uranium removal by zero valent iron may occur via adsorption onto iron corrosion products, and by reduction to less soluble valence states by reactions with elemental iron. This research investigated the effects of water chemistry and surface precipitate buildup on the removal of soluble uranium by zero valent iron. Batch testing was performed to assess solution chemistry effects on uranium adsorption to the potential iron corrosion products, magnetite and a mixed valent amorphous iron oxide. Uranium adsorption to the simulated iron corrosion products was highly dependent on pH, and the concentration and speciation of the background electrolyte solution. Uranium removal via reduction by elemental iron closely approximated pseudo-first-order removal kinetics, despite the buildup of up to 40,000 monolayers of precipitated uranium on the iron surfaces. This indicates that the rate of uranium removal is not strongly dependent on the thickness of the adsorbed uranium layer. Short-term rates of uranium reduction were similar for all solutions tested, but long-term rates were highly dependent on water chemistry. Compared to deionized water, uranium removal rates were increased in sodium chloride containing solutions and reduced in sodium nitrate solutions. The strong influence of water chemistry on long-term reduction rates indicates that system design will require extnded testing with the ground water of interest.

Introduction

Iron mediated reductive precipitation of redox active metal species has been proposed as a method for removing soluble metals and radionuclides from contaminated ground water (Cantrell et al. 1995). This research investigated the effects of solution chemistry on iron mediated removal of soluble uranium species from contaminated ground water. Past site activities and disposal practices associated with uranium processing operations have resulted in extensive ground and surface water contamination in the Bear Creek Valley (BCV) watershed in Oak Ridge, Tennessee. Presently, there is no practical remediation protocol for ground water contaminated by soluble uranium. In most instances, the uranium contamination is accompanied by high levels of other regulated metals and nitrate, thus reducing the effectiveness of ion exchange and adsorption processes for remediation of this water.

Uranium in ground water environments may exist in one of several oxidation states, depending on the local redox conditions. In surface and shallow ground water, uranium is most commonly found in its hexavalent oxidation state as the uranyl ion (UO_2^{2+}), while under more reducing conditions, uranium may be reduced to its tetravalent oxidation state, (UO_2^0). The aqueous solubility of U(VI) may be significantly increased through formation of solubility enhancing complexes with ground water ligands (Langmuir 1978). Carbonate and phosphate are frequently the dominant ligands affecting U(VI) speciation in ground water, and may increase the solubility of U(VI) by several orders of magnitude (Scanlan 1977). In contrast, U(IV) species are much less prone to complexation, and thus ground water ligands generally serve to increase the solubility difference between U(IV) and U(VI) (Shoesmith et al. 1994). The net result of oxidation state and complexation effects is that the aqueous solubilities of U(IV) species range from four to 10 orders of magnitude lower than those of U(VI) (Miyahara 1992). This difference in oxidation state solubilities may be exploited as a mechanism to remove dissolved uranium from contaminated ground water.

Cantrell et al. (1995) reported on the use of zero valent iron for removal of soluble uranyl species from aqueous solution. Removal of soluble uranium was attributed to reductive precipitation of U(VI) to less soluble U(IV) species, and adsorption of uranyl to iron corrosion products. Several studies have confirmed that iron oxides are effective adsorbents for aqueous uranyl species (Venkataramani et al. 1978; Ford 1992; Theis et al. 1994; Payne and Waite 1991; Ho and Miller 1986; Hsi and Langmuir 1985).

A recent investigation has confirmed that zero valent iron can reduce uranium species adsorbed on its surface (Fiedor et al. 1998). Using X-ray photoelectron spectroscopy (XPS), Fiedor et al. (1998) found that uranyl reduction occurred only under anaerobic conditions, but not all of the uranium associated with the iron surfaces was in the U(IV) valence state. Under anaerobic conditions, the thermodynamics of U(VI) reduction by zero valent iron can be described by the redox couples (Pourbaix 1966):

$$UO_2^{2+} + 2e^- = UO_2^0 \qquad E = 0.221 + 0.0295 \log [UO_2^{2+}] \quad (1)$$

$$Fe^0 = Fe^{2+} + 2\,e^- \qquad E = 0.44 - 0.0295 \log [Fe^{2+}] \quad (2)$$

[a]Department of Chemical and Environmental Engineering, University of Arizona, Tucson, AZ 85721.

[b]Midwest Research Institute, East Tennessee Technology Park, Oak Ridge, TN 37831-7274.

[c]Bettis Atomic Power Laboratory, Westinghouse Electric Co., West Mifflin, PA 15222.

Received September 1998, accepted February 1999.

Table 1
Properties of the Iron Oxide Adsorbents

Material	Description	Surface Area (m^2/g)
Alfa magnetite	crystalline Fe_3O_4	5.6
Alfa hematite	crystalline Fe_2O_3	9.4
Isaac mixed oxide	amorphous Fe(II)/Fe(III)	9.6

The equilibrium potential for the overall cell reaction is then given by

$$E = 0.661 + 0.0295 \log [UO_2^{2+}] - 0.0295 \log [Fe^{2+}] \quad (3)$$

Under conditions of environmental interest, the cell potential in Equation 3 is positive, and thus reduction of U(VI) by zero valent iron is thermodynamically favorable.

Knowledge of uranium reduction kinetics and the adsorptive properties of iron corrosion products are essential in designing a practical remediation system using iron media. To that end, the goals of this investigation were to determine the effects of water chemistry on uranium reduction kinetics, and on uranium adsorption by iron corrosion products. Although the adsorption behavior of uranyl on the iron oxides goethite, hematite, and hydrated ferric oxide has been studied previously by other investigators (Payne and Waite 1991; Ho and Miller 1986; Hsi and Langmuir 1985), the corrosion products in an anaerobic iron treatment system are likely to include magnetite and amorphous ferrous and ferric hydroxides (Grambow et al. 1996). Since significant differences in adsorption behavior have been found among different iron oxide materials (Hsi and Langmuir 1985), this research investigates the adsorption behavior of uranyl on magnetite, and on a mixed valent amorphous iron oxide. Rates of uranyl reduction by zero valent iron coupons were also determined to assess the effects of precipitate buildup and iron surface passivation on long-term uranium removal rates.

Materials and Methods

Adsorption Studies

The potential for adsorption of aqueous uranyl species onto iron corrosion products was assessed using magnetite and an amorphous mixed valent iron oxide as simulated iron corrosion products. For comparative purposes, uranyl adsorption on hematite was also measured. Properties of the iron oxide adsorbents are listed in Table 1. The specific surface areas were measured via nitrogen adsorption using the method of Brunauer, Emmett, and Teller (BET) (Brunauer et al. 1938). Crystalline magnetite and hematite were obtained from Alfa/Aesar (Ward Hill, Massachusetts) and the amorphous mixed valent iron oxide was obtained from Isaac Materials (Phoenix, Arizona).

The adsorption studies were performed by placing 50 mg of iron oxide material into 10 mL of test solution contained in 10 mL glass screw top vials. The test solutions were prepared from 3.9 mM uranyl nitrate stock solutions containing the gamma emitting isotope U^{233} at a level of 0.034 mM. The stock solutions were diluted with deionized water to achieve final uranium concentrations of 0.39 mM. Solutions with initial pH values between 2 and 10 were prepared by adding concentrated hydrochloric acid or sodium hydroxide before addition of the iron oxides. Addition of the iron oxides to the test solutions resulted in pH changes of approximately one pH unit. The pH increased in solutions with initial pH values less than eight, but decreased in solutions with initial pH values greater than eight. After equilibration periods of one day, final solution pH values were measured with an Orion gel-filled pH probe. Sampling at shorter time intervals indicated that adsorption equilibrium was reached in less than one hour. Aqueous concentrations were determined by withdrawing 2 mL samples using disposable plastic syringes fitted with 0.2 μm Acrodisc polypropylene filters (Nalgene). At each pH value, filtered and unfiltered control experiments containing no iron oxide adsorbent indicated that uranium losses due to adsorption on the filters and syringes were negligible. Analyses of U^{233} solutions were performed by gamma counting on a Packard Auto-Gamma, Model 500 instrument.

The solutions used in this investigation included two ground water samples from the BCV aquifer and three simulated ground water samples prepared in the laboratory. The two natural ground water samples varied widely in composition and ionic strength as a result of differing contamination sources. Table 2 lists the major inorganic components of ground water type 1 (GW-1) and 2 (GW-2). Metal ion concentrations were determined using inductively coupled plasma (ICP) analysis employing EPA method SW848-6010A. Anion analyses were performed using ion chromatography with EPA method 300.0. Prior to use, the GW-1 and -2 samples were filtered with 0.2 μm polypropylene filters (Nalgene) to remove any suspended sediments.

Reduction Studies

Experiments investigating reduction of aqueous uranyl species were conducted under anaerobic conditions in 500 mL polypropylene containers. Under anaerobic conditions, iron corrosion rates are greatly diminished compared to those under aerobic conditions, and the predominant iron corrosion product is ferrous iron (Uhlig and Revie 1985). Since ferrous iron is several orders of magnitude more soluble than ferric iron, the anaerobic conditions minimized the formation of iron hydroxide colloids in the batch reactors. Anaerobic conditions were maintained by purging the solutions with nitrogen gas at 20 mL/min through 16 mm O.D., type 316 stainless steel tubing inserted through the bottle caps. The purge gases were vented through a second piece of 16 mm stainless steel tubing. Purging the solutions with dry nitrogen resulted in loss of ~15 mL of water from the test solutions during the month long experiment. Calculations of the uranium mass removed from solution were adjusted accordingly to account for this loss of water.

The test solutions were prepared by adding 50 mL of 3.9 mM uranyl nitrate stock solution to 450 mL of either GW-1, GW-2, deionized water, 0.4 M NaCl, or 0.4 M $NaNO_3$ solutions. The background electrolyte concentration of 0.4 M was selected for the ground water simulants in order to approximate the highest observed ionic strength of water from the GW-1 source area. NaCl and $NaNO_3$ were selected for their high aqueous solubilities as sources of chloride and nitrate. Baxter pH test strips, color calibrated in increments of 0.1 pH units, were used for pH determination.

Iron coupons punched from mild steel plate measuring 1.43 cm in diameter by 0.15 cm in thickness were used as the zero valent iron reactants. The coupons contained trace impurities of aluminum and silicon, as determined by wave dispersive X-ray fluorescence. A previous investigation with these coupons determined that the coupon surfaces were coated with iron oxides and small amounts of carbon (Fiedor et al. 1998).

Table 2
Select Characteristics of Filtered BCV Ground Water Types 1 and 2
(Values represent averages of two analyses)

Property	Ground Water 1	Ground Water 2
pH	5.92	6.84
Carbonate (mg/L)	92	96
Calcium (mg/L)	2035	52
Sodium (mg/L)	497	8
Magnesium (mg/L)	360	5.9
Manganese (mg/L)	135	0.82
Potassium (mg/L)	45	6
Barium (mg/L)	17	0.12
Aluminum (mg/L)	4.7	0.08
Nickel (mg/L)	3.7	<0.025*
Cadmium (mg/L)	0.33	0.004
Zinc (mg/L)	0.10	0.055
Uranium (mg/L)	0.008	0.24
Nitrate (mg/L)	10,170	<1*
Chloride (mg/L)	241	13
Nitrite (mg/L)	45	<1*
Fluoride (mg/L)	43	<5*
Sulfate (mg/L)	32	23

*Method detection limit.

The advantage of using coupons in lieu of iron filings is that their reactive surface area can be more accurately determined than that for irregularly shaped iron filings. As indicated in Table 1, iron oxides have high specific surface areas, and thus even small amounts of surface associated oxides will interfere with measurement of the zero valent reactive surface area. Thus, for iron coated with iron oxides, the BET measured surface area may greatly exceed the reactive surface area. Therefore, the nominal geometric surface area may provide a more accurate assessment of the reactive surface area than the surface area measured via BET analysis.

In the uranium reduction experiments, a single iron coupon was placed in 500 mL of test solution after deoxygenating the solutions via nitrogen purging. This methodology resulted in a large solution volume per reactive surface area, and was chosen to: (1) minimize adsorption as a removal mechanism; (2) minimize pH changes associated with corrosion of the iron; and (3) allow a thick buildup of precipitated uranium on the iron surfaces.

Results

Uranyl Adsorption

The adsorbed/aqueous phase partitioning coefficient (K_d) for uranyl uptake by three iron oxide materials from GW-2 is illustrated in Figure 1 as a function of the final pH value. As used here, the uranyl K_d is a lumped parameter which incorporates both specific adsorption via ligand exchange, electrostatic adsorption, and possibly surface precipitation. Additionally, the K_d value is expected to be concentration dependent, due to saturation of specific adsorption sites with increasing uranyl concentration. Specific adsorption of uranyl to iron oxides has been characterized in terms of surface complexation reactions of uranyl hydroxide and uranyl carbonate species with the oxide surface species FeO^- and $FeOH_2^+$ (Hsi and Langmuir 1985; Ho and Miller 1986; Payne and Waite 1991).

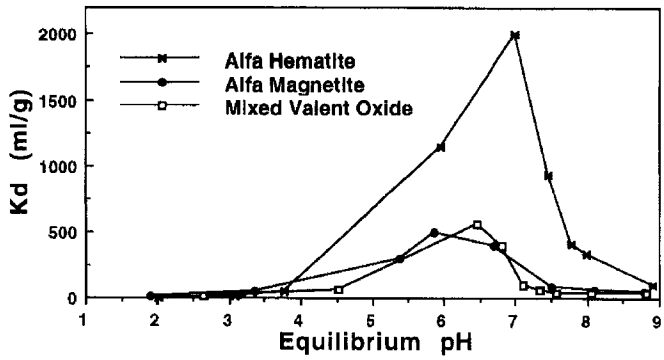

Figure 1. Uranium adsorbed/aqueous phase distribution coefficient (K_d) for hematite, magnetite, and a mixed valent iron oxide from GW-2 as a function of pH.

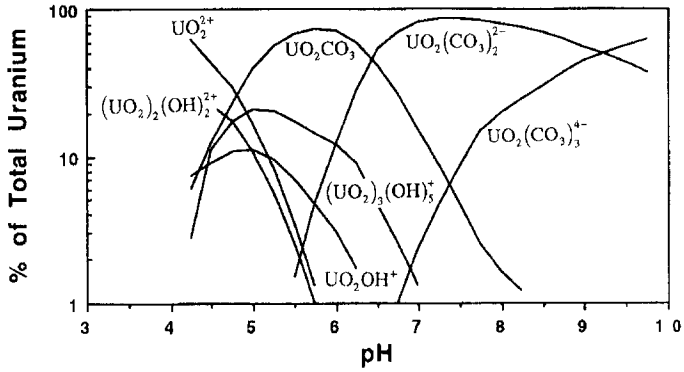

Figure 2. Speciation of dissolved uranium in GW-2 as function of pH as determined by MINTEQA2 using the components listed in Table 2. Species accounting for less than 5% of the total uranium concentration have been omitted from the graph.

Mechanistic descriptions of this type require knowledge of the number, charge, and uranyl affinity of the surface sites as a function of pH. Unfortunately, a detailed description of this type is not possible for iron corrosion products given that both the amount and structure change with time. The initially formed amorphous corrosion products are often metastable with respect to other oxide phases. For example, hydrous ferrous oxide may be transformed into magnetite, goethite, lepidocrocite, or maghemite under conditions relevant to ground water treatment systems (Cornell and Schwertmann 1996). Determination of which stable oxide forms depends on the pH, the redox conditions, and the rate at which oxidation takes place.

Although surface complexation modeling is beyond the scope of this work, it is worthwhile to qualitatively understand the adsorption behavior exhibited in Figure 1. The effect of pH on uranyl adsorption is similar on all three oxide materials. This indicates that uranium adsorption onto potential iron corrosion products can be understood in terms of the behavior exhibited by the well studied uranyl-hematite system. All three oxide materials show a maximum in K_d between pH 6 and 7, a trend is similar to that reported by Ho and Miller (1986) and Hsi and Langmuir (1985) for adsorption of uranyl carbonate complexes on hematite. The strong dependence of adsorption on pH can be explained by changes in the iron oxide surface charge and uranyl speciation with pH. For iron oxide materials, the pH at which there is no net charge on the oxide surface is typically in the range of 6 to 8.5 (Silva and Nitsche 1995). Higher pH values increase the number of negatively charged sites, whereas lower pH values increase the number of positively charged sites. Not

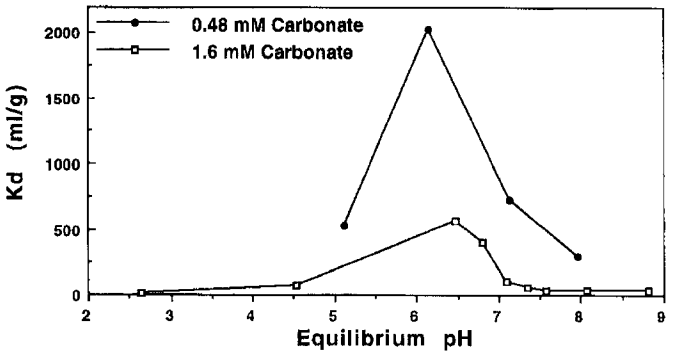

Figure 3. The effect of carbonate concentration on adsorption of uranyl to a mixed valent iron oxide material as a function of pH in GW-2.

only is the oxide surface charge a function of pH, but the speciation of the dissolved uranyl also depends on pH.

The effect of pH on the speciation of the aqueous uranyl was investigated using the thermodynamic equilibrium model, MINTEQA2 (U.S. EPA 1991). Prior to use, the equilibrium constants in the model's database were checked against published sources (Langmuir 1978). Modeling results for the GW-2 solution are shown in Figure 2. At pH values below 5, aqueous uranyl exists primarily as positively charged complexes, while at pH values greater than 7, negatively charged complexes dominate the uranyl speciation. The adsorption behavior exhibited in Figure 1 can be then be explained by the fact that the iron oxides and uranium complexes carry the same charge at both low and high pH. In the pH range where the maximum adsorption occurs, the carbonate complexes $UO_2CO_{3\,(aq)}$ and $UO_2(CO_3)_2^{2-}$ are the predominant uranyl species, and their adsorption likely accounts for most of the uranium uptake. This finding is similar to that reported by Payne and Waite (1991) for uranyl adsorption onto hydrous ferric oxide. In the pH range 6 to 7, uranium adsorption was attributed to formation of $FeOH_2^+ - UO_2CO_3$ and $FeOH_2^+ - UO_2\,(CO_3)_2^{2-}$ surface complexes.

Because carbonate complexation dominates the speciation of dissolved uranium, uranyl adsorption by iron corrosion products should be highly dependent on the carbonate concentration. The effect of carbonate concentration on uranyl adsorption was investigated using GW-2 and the mixed valent amorphous oxide. For this experiment, the total carbonate concentration of the GW-2 sample was reduced from its initial value of 1.6 mM to 0.48 mM by purging the solution with nitrogen gas for seven days. Figure 3 compares uranyl adsorption onto the mixed valent oxide from the low and native carbonate GW-2 solutions. In the lower carbonate solution, the maximum uranyl K_d of 2000 mL/g is more than three times the maximum observed value of 540 mL/g in the native carbonate sample. MINTEQA2 solution modeling shows that reducing the solution carbonate concentration at pH 6 leads to an increase in concentration of $(UO_2)_3\,(OH)_5^+$ from 12% to approximately 35% of the total uranium. Correspondingly, the total concentration of the uranyl carbonate complexes decreases from 84 to 57% of the total uranium. This suggests that on the mixed valent oxide, adsorption of uranyl carbonate complexes is weaker than adsorption of uranyl hydroxyl complexes, and that adsorption of $(UO_2)_3\,(OH)_5^+$ is responsible for the increased uptake observed in the low carbonate sample. This finding is in agreement with a previous investigation using goethite and hydrous ferric oxide which found that $(UO_2)\,OH^+$ and $(UO_2)_3\,(OH)_5^+$ adsorb preferentially to UO_2CO_3 and $UO_2\,(CO)_2^{2-}$ complexes (Hsi and Langmuir 1985).

Competitive adsorption by background electrolytes was also found to affect uranyl uptake by iron oxides. Comparisons of uranyl uptake from GW-1 and -2 indicated that the Kd values for adsorption from GW-2 were approximately twice those for adsorption from the higher ionic strength GW-1. This indicates that uranyl adsorption to iron corrosion products is subject to competition by other electrolytes.

Uranyl Reduction

Although ferrous ions can reduce U(VI) in concentrated acid solutions (Baes 1953; Katz and Rabinowitz 1951; Grambow et al. 1996), iron mediated reduction of U(VI) under environmental conditions requires zero valent iron, and is therefore a surface mediated reaction. Surface mediated reactions following first order kinetics can be described in terms of a first order rate constant. The observed first order rate constant (k_{obs}) may be defined as

$$k_{obs} = -\frac{d(\ln C/C_o)}{dt}\frac{V_s}{S} \qquad (4)$$

where C_o is the initial reactant concentration, C is the reactant concentration as a function of time (t), V_s is the solution volume (500 mL), and S is the reactive surface area (3.8 cm^2). The rate constant defined in this manner is normalized to a surface area to solution volume ratio of 1 cm^2/mL, and can be compared easily to rate constants determined under other experimental conditions. Since the observed first order rate constant may be affected by mass transfer limitations, it must be distinguished from the intrinsic rate constant, k, which expresses the kinetics of the surface mediated reaction in the absence of mass transfer limitations.

Figure 4 compares data for uranium removal by iron coupons in GW-1 and -2, and shows that uranium removal in the two ground water samples displayed significantly different kinetics. Uranium removal in the GW-1 solution was associated with formation of a yellow colored precipitate. Although much of this precipitate settled to the bottom of the solution, comparison of filtered and unfiltered samples at one week elapsed indicated that 20% of the initially added uranium was present as suspended particulates. XPS analysis of the precipitate indicated that it contained uranium in the U(VI) valence state as well as high concentrations of calcium. Gamma counting 32 mg of this wet precipitate indicated that it contained 9.6 mg of uranium. MINTEQA2 modeling indicates that at pH values greater than 5.5, the GW-1 solution is supersaturated with respect to barite ($BaSO_4$), fluorite (CaF_2), and ruthefordine (UO_2CO_3). This suggests that the precipitate may be a mixture of fluorite and ruthefordine. Although the pH of the GW-1 solution was 5.9 at the start of the experiment, as shown in Figure 5, no precipitates were observed prior to addition of the iron coupon. Since addition of the iron coupon did not affect the solution pH, this suggests that the surface of the iron coupon served to nucleate precipitation of the supersaturated species.

As shown in Figure 4, uranium concentrations in the GW-2 solution showed a rapid initial drop in the first four hours of the experiment, followed by a more gradual decline during the remainder of the test. After the first four hours, uranium removal from GW-2 approximated first-order kinetics. MINTEQA2 solution modeling suggests that the initial drop in solution concentration resulted from precipitation of schoepite ($UO_3{*}2H_2O$), which is

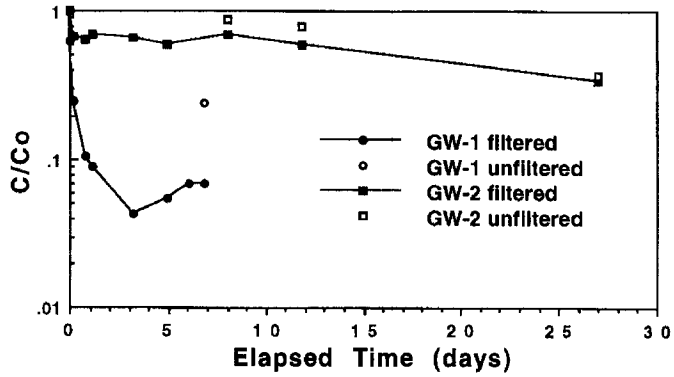

Figure 4. Uranium removal from 500 mL anaerobic solutions of GW-1 and -2 by zero valent iron coupons.

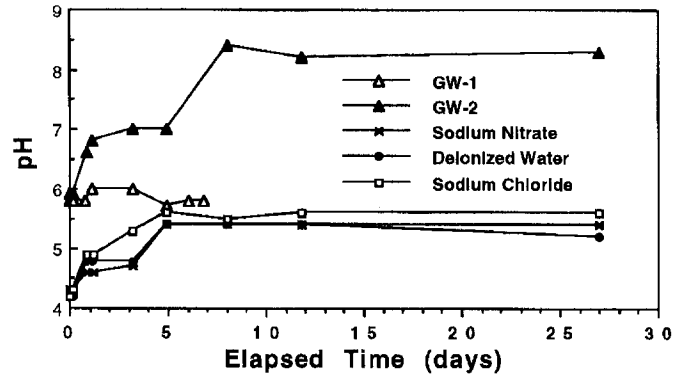

Figure 5. pH variations in anaerobic iron coupon experiments.

predicted to occur at pH values above 5.5. The modeling prediction of precipitate formation was supported by data from unfiltered samples taken at 7.6 and 11 days elapsed, as shown in Figure 4. Comparison of filtered and unfiltered samples indicated that 21% of the total uranium was associated with suspended particulates. However, after 650 hours elapsed, uranium concentrations in filtered and unfiltered samples differed by only 1.3%, indicating the removed uranium was associated with the iron coupon.

Uranium removal kinetics from the three ground water simulants are compared in Figure 6. In each solution, the rate of uranium removal was fastest during the initial 24 hours of the test, and closely approximated first-order behavior during this period. First-order rate constants were calculated using least squares regression analyses for the GW-2, deionized water, NaCl, and $NaNO_3$ solutions. The observed first day rate constants and the average rate constant from days 2 through 30 are presented along with their regression correlation coefficients in Table 3. The observed first day rate constants for the deionized water, NaCl, and $NaNO_3$ solutions indicated similar rates of uranium removal from all three solutions. However, the average rate constants during days 2 through 30 indicate a difference of more than a factor of 10 in uranium removal rates between the NaCl and $NaNO_3$ solutions. In the NaCl solution, the observed rate constant decreased by a factor of ~3 between days 1 and 30; whereas for the $NaNO_3$ solution, the rate constant declined by a factor of 35 during this period.

Comparison of filtered and unfiltered samples from the ground water simulant solutions indicated that all the uranium removal was associated with the iron coupons. In these solutions, the maximum difference in uranium concentrations between filtered and unfiltered samples was less than 1% of the initial uranium concentration. This result confirms the absence of suspended iron corrosion products as an adsorbent material, and confirms that the removal mechanism is adsorption/reduction at the iron coupon surface. XPS analysis of iron coupons from similar experiments in a previous investigation confirmed reduction of uranyl to U(IV) (Fiedor et al. 1998).

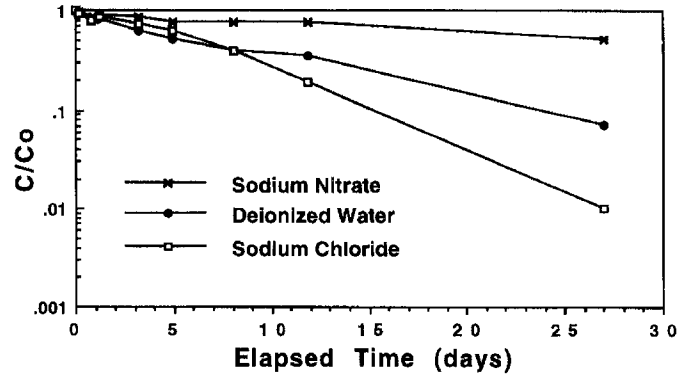

Figure 6. Removal of soluble uranium from 500 mL solutions of 0.4 M $NaNO_3$, deionized water, and 0.4 M NaCl by iron coupons under anaerobic conditions.

The effect of mass transfer limitations on the observed rate constants in Table 3 was investigated by determining the mass transfer rate constant for aerobic corrosion of the iron coupons in solutions purged with air at 20 mL/min. Because iron corrosion by dissolved oxygen is limited by the rate of diffusive mass transfer (Uhlig and Revie 1985), the rate of iron corrosion in air purged solutions can be used to estimate the mass transfer coefficient for diffusion through the hydrodynamic boundary layer surrounding the iron coupons. The rate of iron corrosion was determined by measuring the increase in aqueous iron concentrations (Fe_{aq}) in three air purged solutions. Measurements of dissolved iron concentrations as a function of time (t), along with the aqueous diffusion coefficient for dissolved oxygen ($D^{O_2}_{aq}$), can be used to determine the thickness of the film boundary layer (δ) surrounding the iron coupons, from Sherwood et al. (1975):

$$\frac{d(Fe_{aq})}{dt} = \frac{D^{O_2}_{aq}}{\delta}\left(C^{O_2}_{b} - C^{O_2}_{s}\right) \qquad (5)$$

where $C^{O_2}_{b}$ is the molar concentration of oxygen in the bulk solution, and $C^{O_2}_{s}$ is the oxygen concentration at the coupon surface. Assuming an instantaneous surface reaction where $C^{O_2}_{s}$ is zero, and $C^{O_2}_{b}$ is equal to the solubility of oxygen in water (9 mg/L), an upper bound estimate of the boundary layer thickness can be calculated. Averaging the results from three aerobic corrosion tests yielded a maximum boundary layer thickness of 67 μm. This boundary layer thickness can then be used to calculate the mass transfer coefficient (k_f) for uranyl in the nitrogen purged experiments, from Sherwood et al. (1975):

$$k_f = \frac{D^{UO_2^{2+}}_{aq}}{\delta} \qquad (6)$$

Using a D_{aq} for uranyl of 6.52 × 10^{-6} cm^2/s (*Gmelin Handbook of Inorganic Chemistry* 1984) and a boundary layer thickness of 67 μm yields a mass transfer coefficient for uranyl of 5.9 × 10^{-2} cm/min. Since this value is only 2.4 times the maximum observed rate constant of 2.5 × 10^{-2} cm/min in Table 3, the observed removal rates

Table 3
First-Order Removal Rate Constants and their Associated Correlation Coefficients for the Data Depicted in Figures 4 and 6

Water	Day 1 Rate Constant (cm/min)	R^2	Days 2 to 30 Rate Constant (cm/min)	R^2
GW-2	4.4×10^{-2}	0.615	2.3×10^{-3}	0.859
D.I. water	2.5×10^{-2}	0.985	3.5×10^{-3}	0.987
0.4 M NaCl	2.5×10^{-2}	0.960	7.9×10^{-3}	0.987
0.4 M $NaNO_3$	2.5×10^{-2}	0.984	7.2×10^{-4}	0.920

during the first day of reaction may be influenced by mass transfer limitations. However, for the data obtained from days 2 through 30, the mass transfer coefficient for UO_2^+ ranges from 7.5 to more than 80 times the observed rate constants. Thus, the measured rate constants during this period are indicative of surface reaction rates rather than mass transfer limitations.

Differences in performance among the test solutions cannot be attributed to differences in U(IV) solubility, since the solubility of $UO_{2\,(aq)}$ is only weakly affected by the solution chemistry (Shoesmith et al. 1994). Also, pH effects cannot explain the differences in removal rates among the three simulant solutions, since similar pH behavior was observed, as indicated in Figure 5. Therefore, the performance differences shown in Figure 6 are due to a specific effect of the electrolytes in each solution. If deionized water is taken as the baseline case, the data in Figure 6 indicate that chloride ions enhance the rate of uranium removal while nitrate ions reduce uranium removal rates. However, the similar rates observed during the first day of reaction indicate that the effect of these anions manifests itself only over an extended period of time.

The effect of chloride and nitrate on the reactivity of iron in anaerobic solutions was investigated by measuring the open circuit potential of an iron wire electrode placed in anaerobic solutions of varying chloride and nitrate concentrations. A platinum wire was used as the counter electrode, and the iron potentials were measured versus a silver/silver chloride reference electrode. Figure 7 shows the open circuit potential of the iron wire referenced to the standard hydrogen electrode. In the nitrate solutions, the open circuit potential increased with increasing nitrate concentration, indicating that nitrate is acting as an oxidant. Thus, the decreased uranium removal rate in the nitrate solution may be attributed to the oxidizing activity of nitrate, which may inhibit or compete with the reduction of U(VI), and may enhance passivation of the iron surfaces by increasing the formation of iron oxides. As shown in Figure 7, chloride had the opposite effect of nitrate on the open circuit potential of the iron. The decreasing potential with increasing chloride concentration indicates that the iron is more actively corroding at higher chloride concentrations. Investigations of iron corrosion behavior indicate that chloride ions promote enhanced corrosion by increasing the porosity of surface associated oxide layers (Trethewey and Chamberlain 1988). Therefore, the increased rate of uranium removal in the chloride containing solutions may be attributed to greater access of the uranyl ions to the reactive surface. The data in Figure 7 also show that the corrosion enhancing effect of chloride ions is most pronounced at chloride concentrations below 50 mM.

As indicated by the correlation coefficients listed in Table 3, rates of uranium removal during days 2 through 30 closely approximated first-order behavior. This is a surprising result given the increasing thickness of the surface adsorbed precipitate layer over the course of the experiments. After 30 days elapsed, the thickness of the uranium layer on the iron coupon in the NaCl solution is calculated to be 15 μm thick, or 40,000 monolayers, based on a density of 9.35 g/mL for UO_2 as the surface precipitate (*Gmelin Handbook of Inorganic Chemistry* 1984). This suggests that the rate of uranium removal is not strongly dependent on the thickness of the surface associated precipitation layer.

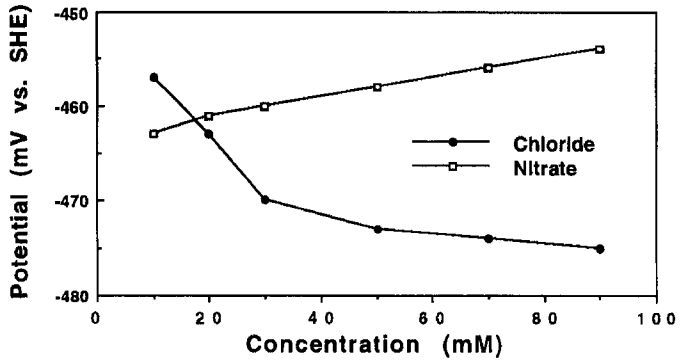

Figure 7. Open circuit potential versus the standard electrode (SHE) of an iron wire placed in anaerobic solutions of sodium nitrate and sodium chloride.

The independence of the uranium removal rate on the thickness of the adsorbed uranium layer may result from the fact that the uranium on the coupon surfaces is hyperstoichiometric UO_2, which is an electrically conductive oxide (Shoesmith et al. 1994). In previously reported results, XPS indicated that the stoichiometry of uranium on the coupons corresponds to $UO_{2.25}$, which is hyperstoichiometric in oxygen with respect to UO_2 (Fiedor et al. 1998). Hyperstoichiometric UO_2 has the same cubic fluorite structure as UO_2, but contains interstitial O^{2-} ions that contribute to its high electrical conductivity (Shoesmith et al. 1994). The presence of an electrically conductive surface coating may allow efficient transfer of electrons from the iron to adsorbed U(VI).

Discussion

Under anaerobic conditions, zero valent iron is capable of reducing U(VI) to a less soluble oxidation state. However, the data in Figures 4 and 6 indicate that slow reaction kinetics may require a treatment system with a long hydraulic residence time. Removal half-lives in a flow-through system can be estimated from the observed rate constants listed in Table 3. Extrapolation of the batch data to packed bed conditions can be made by adjusting the observed rates of uranium removal for differences in reactive surface area per volume of solution. As measured in our laboratory, a column packed with 40 mesh iron filings contains 5 g of iron per milliliter of solution volume. Assuming spherical granules, the geometric surface area of these filings is 0.80 cm^2/g. This yields a geometric surface area to solution volume ratio of 4.0 cm^2/mL for a packed bed of 40 mesh filings. Thus, the half-life ($t_{1/2}$) in a packed bed of 40 mesh iron filings can be estimated from the observed rate constant as

$$t_{1/2} = \frac{\ln(2)}{k_{obs} \times 4\ cm/mL} \qquad (7)$$

Table 4
Estimated Solution Half-Lives and 90% Removal Times for Uranium in a Packed Bed of 40 Mesh Iron Filings Based on Extrapolation of Batch Test Rate Constants Measured Between Days 2 and 30 Elapsed

Solution	Removal Half-Life (min)	Time for 90% Removal (min)
0.4 M $NaNO_3$	98	324
GW-2	77	254
Deionized	21	71
0.4 M NaCl	9.6	32

Table 4 lists the estimated removal half-lives in a packed bed of 40 mesh iron filings for each solution composition. Also listed in Table 4 are the hydraulic residence times required to achieve an order of magnitude reduction in aqueous uranium concentrations, based on the estimated half-lives. Because of capital cost considerations, unit operations such as carbon adsorption or ion exchange typically operate with hydraulic residence times ranging from 10 to 20 minutes (Reynolds and Richards 1996). Thus, the required residence times listed in Table 4 indicate that uranium reduction by zero valent iron may be too slow for use in aboveground canister systems, but may be feasible for in situ applications where treatment zone residence times may be much greater.

Although the half-life estimates in Table 4 appear to make zero valent iron a potentially practical remediation technology for removing soluble uranium, the adsorption studies suggest that several factors may complicate its application to field sites. The strong influence of water chemistry on adsorption of uranium to iron corrosion products may be a serious problem if a change in ionic strength, pH, or carbonate concentration leads to release of adsorbed uranium from the treatment zone. Additionally, the sloughing of iron corrosion products from the treatment zone may contribute to colloidal transport of adsorbed uranium.

The strong influence of water chemistry on rates of uranium reduction indicates that system design will require laboratory testing with the ground water of interest. This testing, however, will be complicated by the slow manifestation of solution chemistry effects on uranium removal rates. Thus, long-term testing will be required to predict long-term system performance. The batch testing presented here also suggests that column test results will be difficult to interpret due to the confounding influences of the three concurrent removal mechanisms of reduction, adsorption, and coprecipitation.

Acknowledgments

The authors would like to thank Tie Lie for his assistance with the potential measurements. This work has been authored by a contractor of the U.S. Government under contract DE-AC05-840R21400. Accordingly, the U.S. Government retains a paid-up, nonexclusive irrevocable, worldwide license to publish or reproduce the published form of this contribution, prepare derivative works, distribute copies to the public, and perform publicly and display publicly, or allow others to do so, for U.S. Government purposes.

Editor's Note: The use of brand names in peer-reviewed papers is for identification purposes only and does no constitute endorsement by the authors, their employers, or the National Ground Water Associaion.

References

Baes, C.F. Jr. 1953. The reduction of uranium (VI) by ferrous iron in phosphoric acid solution. Oak Ridge National Laboratory Publication No. ORNL1581. Oak Ridge, Tennessee: ORNL.

Brunauer, S., P.H. Emmett, and E. Teller. 1938. Adsorption of gases in multimolecular layers. *Journal of the American Chemical Society* 60, no. 2: 309–319.

Cantrell, K.J., D.I. Kaplan, and T.W. Weitsma. 1995. Zero-valent iron for the in situ remediation of selected metals in ground water. *Journal of Hazardous Materials* 42, no. 2: 201–212.

Cornell, R.M., and U. Schwertmann. 1996. *The Iron Oxides*. New York: VCH Publishers.

Fiedor, J.N., W.D. Bostick, R.J. Jarabek, and J. Farrell. 1998. Understanding the mechanism of uranium removal from ground water by zero valent iron using X-ray photoelectron spectroscopy. *Environmental Science and Technology* 32, no. 10: 1466–1473.

Ford, D. 1992. *Toxicity Reduction: Evaluation and Control*. Lancaster, Pennsylvania: Technomic Publishing.

Grambow, B., E. Smailos, H. Geckeis, R. Muller, and H. Hentschel. 1996. Sorption and reduction of uranium (VI) on iron corrosion products under reducing saline conditions. *Radiochimica Acta* 74: 149–154.

Gmelin Handbook of Inorganic Chemistry, 8th ed. 1984. New York: Springer Verlag.

Hsi, C.K.D., and D. Langmuir. 1985. Adsorption of uranyl onto ferric oxyhydroxides: Application of the surface complexation site-binding model. *Geochimica et Cosmochimica Acta* 49: 1931–1941.

Ho, C.H., and N.H. Miller. 1986. Adsorption of uranyl species from bicarbonate solution onto hematite particles. *Journal of Colloid and Interface Science* 110, no. 1: 165–171.

Katz, J.J., and E. Rabinowitz. 1951. *The Chemistry of Uranium: Part I*. New York: McGraw-Hill.

Langmuir, D. 1978. Uranium solution-mineral equilibria at low temperatures with applications to sedimentary ore deposits. *Geochimica et Cosmochimica Acta* 42: 547-569.

Miyahara, K. 1992. Sensitivity of uranium solubility to variation of ligand concentrations in ground water. *Journal of Nuclear Science and Technology* 30, no. 4: 314-332.

Payne, T.E., and T.D. Waite. 1991. Surface complexation modeling of uranium sorption data obtained by isotope exchange techniques. *Radiochimica Acta* 52/53, no. 2: 487-493.

Pourbaix, M. 1966. *Atlas of Electrochemical Equilibria*. Oxford: Pergamon Press.

Reynolds, T.D., and P.A. Richards. 1996. *Unit Operations and Processes in Environmental Engineering*, 2nd ed. Boston, Massachusetts: PWS Publishing.

Scanlan, J.P. 1977. Equilibria in uranyl carbonate systems II. *Journal of Inorganic Nuclear Chemistry* 39, no. 4: 635-639.

Shoesmith, D.W., S. Sunder, and W.H. Hocking. 1994. Electrochemistry of UO_2 nuclear fuel. In *The Electrochemistry of Novel Materials*, ed. J. Lipkowski and P.N. Ross, 297-337. New York: VCH Publishers.

Sherwood, T.K., R.L. Pigford, and C.R. Wilke. 1975. *Mass Transfer*. New York: McGraw-Hill.

Silva, R.J., and H. Nitsche. 1995. Actinide environmental chemistry. *Radiochimica Acta* 70/71, 377.

Theis, T.L., R. Iyer, and S.K. Ellis. 1994. Parameter estimation for trace element sorption on a new granular iron oxide. *Environmental Progress* 13, no. 1: 72–77.

Trethewey, K.R., and J. Chamberlain. 1988. *Corrosion for Students of Science and Engineering*. United Kingdom: Longman Scientific & Technical Publishers.

Uhlig, H.H., and R.W. Revie. 1985. *Corrosion and Corrosion Control*. New York: Wiley-Interscience.

U.S. Environmental Protection Agency (EPA). 1991. MINTEQA2/PRODEFA2: A geochemical assessment model for environmental systems: Version 3 user's manual. EPA/600/3-91/021.

Venkataramani, B., K.S. Ventateswarlu, and J. Shankar. 1978. Sorption properties of oxides III. *Journal of Colloid and Interface Science* 67, no. 2: 187–194.